Thermochimica Acta, 8 (1974) 105–117

A DIFFERENTIAL TEMPERATURE STUDY OF THE THERMAL FUSION OF ADJACENT POLYMER PHASES*

WILLIAM A. FRASER, JOHN C. WHITWELL AND BERNARD MILLER

Textile Research Institute and Department of Chemical Engineering, Princeton University, Princeton, N.J. 08540 (U.S.A.)

(Received 27 August 1973)

ABSTRACT

A differential thermal scanning technique is described for studying the thermally induced disappearance of an interface between thermoplastic materials. This is specifically applicable to the autohesion or self adhesion of thermoplastic polymers.

A mathematical model has been developed to describe the thermal bonding of polypropylene monofilaments (as in certain non-woven processes) which treats bond formation as the disappearance, with heat input, of a thermal contact resistance at the fiber–fiber interface. The predicted results suggest that monitoring the temperature difference across a polymer–polymer interface when a heat flux is applied from one side could be a sensitive means of following bond formation as a function of pressure, temperature, and time.

Experimentally, two polypropylene films with fine wire thermocouples imbedded near their contacting surfaces were bonded using a CO_2 gas laser as a heat source. The observed ΔT data confirmed the general behavior predicted by the model and indicated that only a surprisingly small threshold pressure was necessary to achieve such intimate contact as to significantly influence heat transfer across the interface.

INTRODUCTION

Manufacturing processes utilizing the thermal bonding of polymeric materials have become more prevalent, and their use in the future should be increasing. The production of heat-bonded non-woven fabrics from thermoplastic fibers is one example; others could also be cited. In most cases, adequate bonding must be realized under conditions of temperature, pressure and time which will be least detrimental to inherent polymer or fiber properties. Production technology decisions aimed at meeting these requirements have had to be made by strictly empirical means based on ultimate bond strengths, since little basic information has been available about the bond formation process itself.

---

*Presented at the 4th North American Thermal Analysis Society Meeting, Worcester, Mass., June 13–15, 1973.

This paper presents the concepts and assumptions underlying a mathematical model which predicts the thermal response in the region of a polymer–polymer interface as it disappears on being heated from one side under varying bonding conditions. Based on the predictions of this model, an experimental procedure has been devised for following the changes occurring at the interface during bond formation by laser heating. The technique has been found to be capable of revealing the effects of variations in bonding pressure and adherend surface roughness. Moreover, the experimental results are remarkably consistent with the predictions of the model and, in fact, are interpreted in terms of it.

The experimental system used in this study to fuse or bond thermoplastic polymers incorporated a continuous wave, infrared, CO_2 gas laser, which provides highly localized, precisely controlled heating. Details of this apparatus have been published previously[1]. With this laser, bonding was found to be effected at the intersection between two crossed polypropylene monofilaments extruded so as to have approximately rectangular cross-sections[2–3]. Taking into account the resistance to heat transfer which exists at any solid–solid interface, the mathematical model relates the laser parameters, power density and exposure time, to the temperatures developed throughout such crossed monofilaments during laser heating, bond formation, and subsequent cooling. The predictions of the model suggested a promising and relatively simple thermal analysis technique for following the complicated viscoelastic flow and deformation processes essential for bond formation.

THE HEAT TRANSFER MODEL

As the laser beam impinges on the upper side of the fiber–fiber intersection, depicted in Fig. 1, energy is dissipated by conduction into the filaments and along the filament axes, and by natural convection to the air at filament surfaces. Two orthogonal planes of symmetry section the bond in such a way that the thermal behavior of only one bond quadrant needs to be analyzed. As a further simplification, consideration is restricted to the symmetry plane at $z=0$, so that it is necessary to account for heat conduction in only two spatial dimensions. This model geometry is represented in Fig. 2.

The non-linear partial differential transient heat conduction equation governing filament temperature as a function of time and position in the bond can be written as

$$\rho[C_p(T)+\gamma(T)\Delta H]\frac{\partial T}{\partial t}=K\left[\frac{\partial^2 T}{\partial x^2}+\frac{\partial^2 T}{\partial y^2}\right]+Q_0\alpha e^{-\alpha x}[1-\mathrm{H}(y)]$$

where T = temperature; t = time; x, y = distance in x and y directions, respectively; ρ = density; K = thermal conductivity; α = absorption coefficient of polymer at 10.6 μ wavelength; $C_p(T)$ = heat capacity (a function of temperature); $\gamma(T)\Delta H$ = latent heat term accounting for polymer melting; Q_0 = laser flux at $x=0$; $\mathrm{H}(y)$ = step function with values of 0 or 1, used to denote laser spot size. The temperature-dependent terms, $C_p(T)$ and $\gamma(T)\Delta H$, were evaluated experimentally using differen-

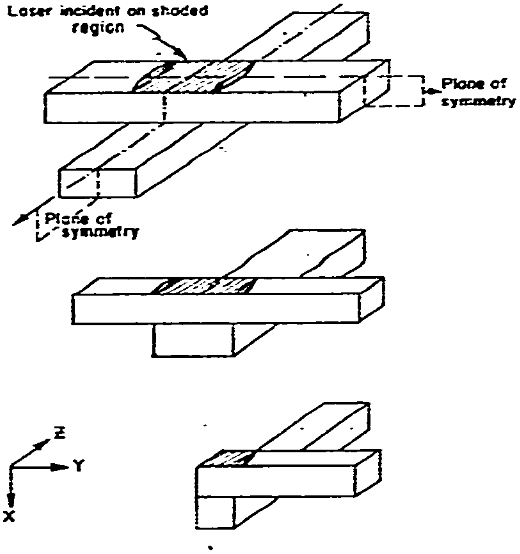

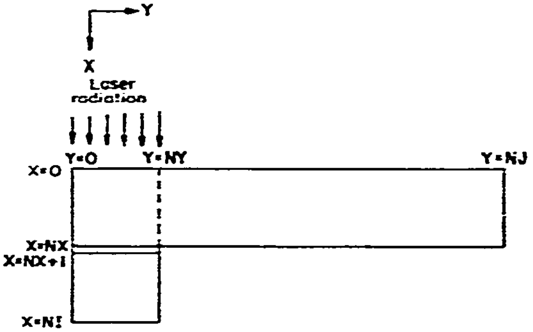

Fig. 1 (left). System geometry and symmetry planes for crossed rectangular monofilaments.

Fig. 2 (right). Two-dimensional model geometry.

tial scanning calorimetry (Fig. 3). Heat capacity is seen to be a linear function of T for both solid and melt, with the latent heat term entering the equation over the temperature range 110–170 °C. The last term of the equation involves the assumption that the absorption of laser energy by the polymer follows Lambert's Law. Here, Q_0 = laser flux (power density) incident on filament surface ($x = 0$) and α = absorption coefficient of polymer at laser wavelength, $10.6\,\mu$, both determined experimentally. In this term $H(y)$ is a step function with values of 0 or 1 used to denote laser spot size. Density, ρ, thermal conductivity, K, and α were assumed independent of T

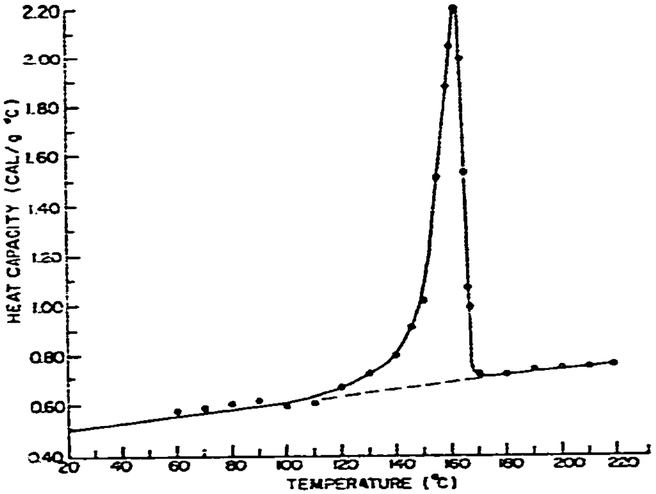

Fig. 3. DSC scan for polypropylene filaments. Heating rate 10 °C/min.

and unchanged in going from solid to melt. While this is not exact, these assumptions are not unreasonable for polymeric materials. Besides, the model is not extremely sensitive to small variations in these parameters.

In setting up the initial and boundary conditions necessary to solve the equation, the assumptions were made that convection losses obey Newton's Law of cooling and that the upper filament is not heated at all at some distance from the intersection ($y = \mathrm{NJ}$) because of the localized laser heating and the low thermal conductivity of polypropylene. Referring to Fig. 2, the initial and boundary conditions necessary to solve the heat conduction equation are:

Initial condition

$$\text{at } t = 0,\ T = T_0 \tag{I.C.}$$

Boundary conditions

$$\text{at } x = 0;\ \frac{\partial T}{\partial x} = h(T - T_0) \tag{B.C. 1}$$

$$\text{at } x = \mathrm{NX},\ y > \mathrm{NY};\ -\frac{\partial T}{\partial x} = h(T - T_0) \tag{B.C. 2}$$

$$\text{at } x = \mathrm{NI},\ y < \mathrm{NY};\ -\frac{\partial T}{\partial x} = h(T - T_0) \tag{B.C. 3}$$

$$\text{at } y = 0;\ \frac{\partial T}{\partial y} = 0 \tag{B.C. 4}$$

$$\text{at } y = \mathrm{NY},\ x > \mathrm{NX};\ -\frac{\partial T}{\partial x} = h(T - T_0) \tag{B.C. 5}$$

$$\text{at } y = \mathrm{NJ};\ T = T_0 \tag{B.C. 6}$$

where T_0 = ambient temperature (25°C); $h = H/K$, where H = heat transfer coefficient for natural convection, K = thermal conductivity of air. The equation was converted to a dimensionless form and solved numerically by the Peaceman–Racheford implicit alternating direction method[4]. To carry out these calculations, a computer program was written incorporating Calcomp plotting routines which present the output as plots of predicted behavior during heating and subsequent cooling. Cooling profiles were calculated by removing the laser source term from the heat transfer equation. The non-linear term which would account for polymer recrystallization, $\gamma(T)\Delta H$, was neglected because of the complexities of localized melting and supercooling, but this omission is not expected to introduce excessive error.

PREDICTED BEHAVIOR—CONTINUUM MODEL

Figure 4 shows how the temperature profile along the central axis of the bond ($y=0$) develops as heating proceeds for the idealized case assuming perfect thermal contact between adjacent surfaces before bond formation, i.e., a continuum. The three-dimensional Calcomp plots of Fig. 5, showing temperature as a function of x and y at $t=4.56$ sec when the interface has reached the melt temperature, illustrate the localization of laser heating due to the low thermal conductivity of polypropylene.

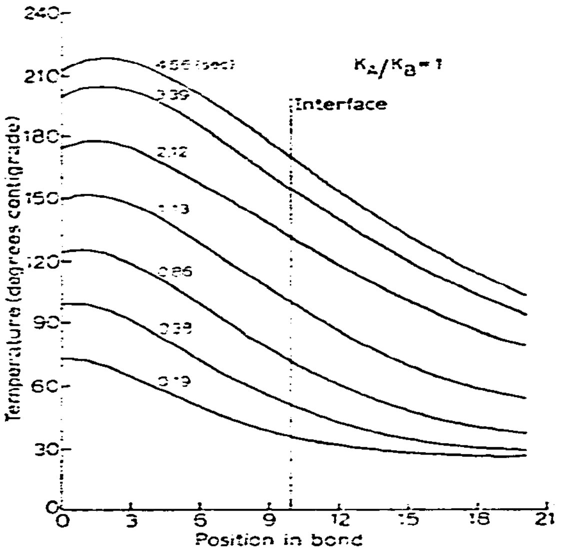

Fig. 4. Predicted temperature profiles developed along central axis of bond at a laser flux of 12 watts/cm^2. Interfacial resistance is ignored. Abscissa units 0.1 × filament thickness.

Figure 6 demonstrates how the predicted temperature profiles along $y=0$ decay on cooling after termination of laser heating. It is seen that cooling is quite rapid, and solidification is expected in the order of 1.4 sec. Figure 7 shows the change in temperature with time at a point on the interface ($x=\mathrm{NX}$, $y=0$) predicted by the continuum model for 4.56 sec of laser heating (to 162°C) followed by cooling.

THE BOND FORMATION MODEL

An interface between two solid layers, even highly polished metal surfaces pressed tightly together, should not be considered a continuum; there is generally a contact resistance to heat transfer. The model can be modified to include this resistance by considering that the thin region at the fiber–fiber interface between $x=\mathrm{NX}$ and $x=\mathrm{NX}+1$ (Fig. 2) consists of an arbitrary gap material of thermal conductivity, K_B, less than that of polypropylene, K_A. The requirements of the numerical technique for solving the heat transfer equation fix the width of the gap;

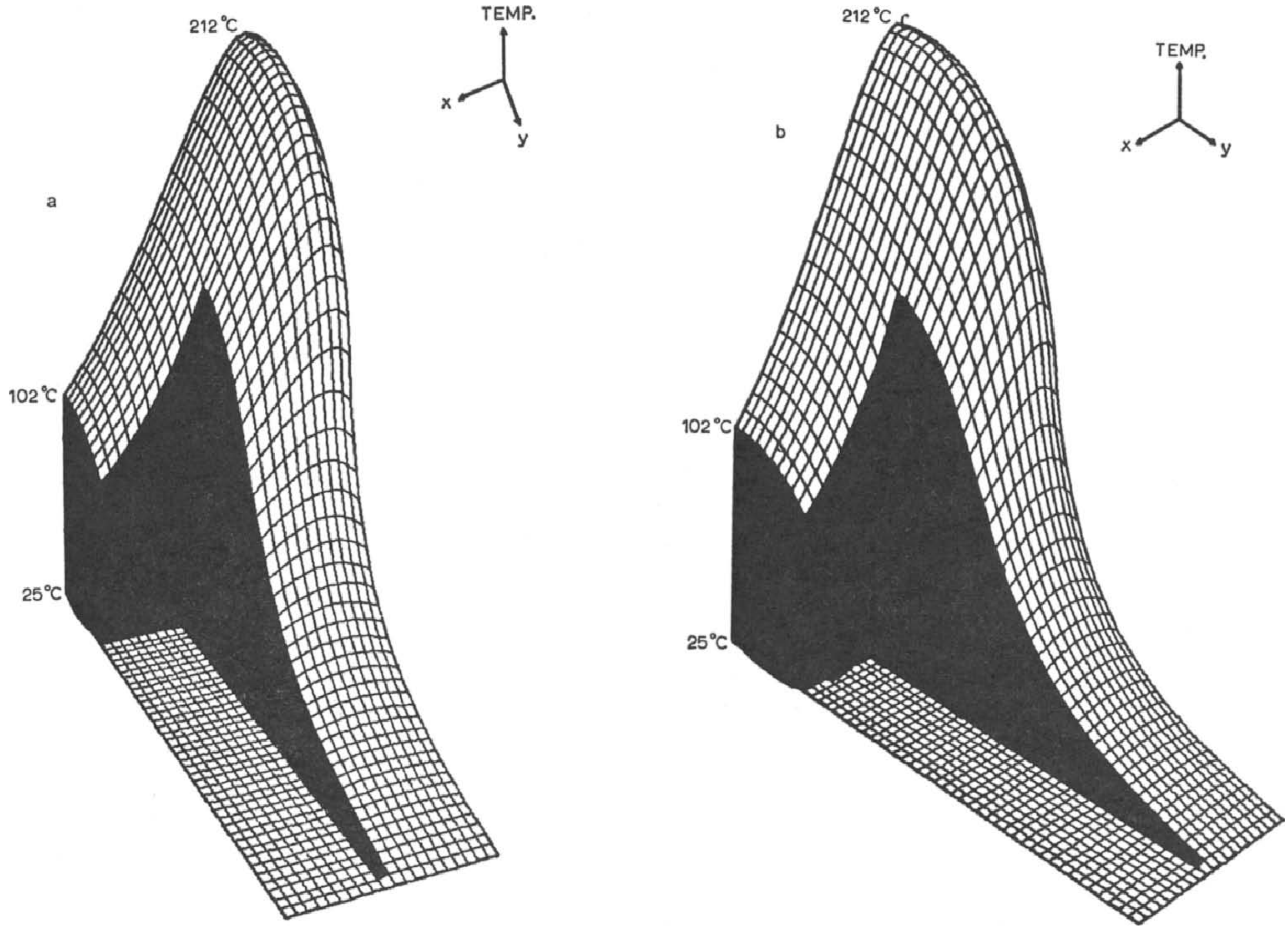

Fig. 5. Three-dimensional computer printouts of the temperature surface $T(x, y)$ at one instant in time when the interface has reached the melt temperature. (a) and (b) are two different projections of the same surface.

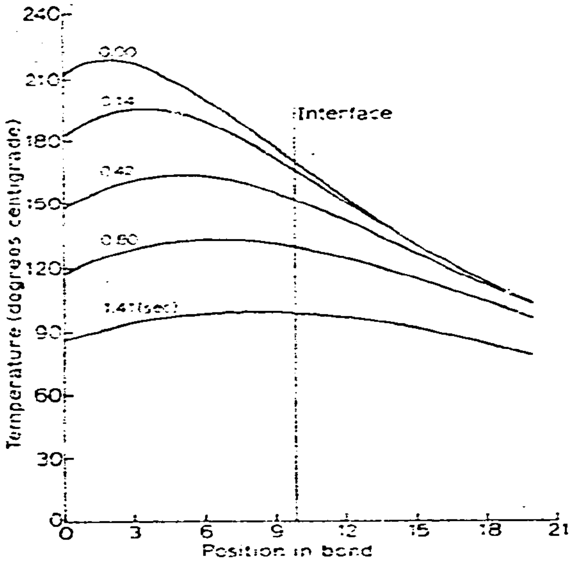

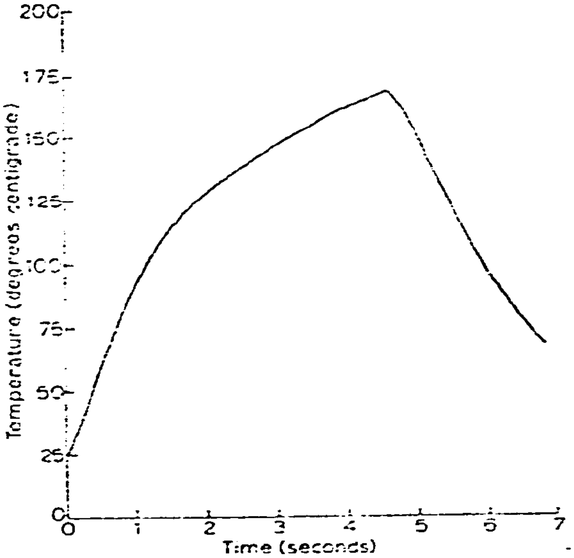

Fig. 6 (left). Predicted temperature profiles developed during cooling. Abscissa units 0.1 × filament thickness.

Fig. 7 (right). Temperature-time behavior for a point at the interface (on lower surface of upper filament) during heating and cooling. Laser flux = 12 watts/cm^2.

consequently, the magnitude of the contact resistance was established by selecting the ratio between the thermal conductivities of polypropylene and the arbitrary gap material.

Bond formation can be modeled as the disappearance of the contact resistance over a temperature range, i.e., $K_B \rightarrow K_A$, where $K_B = F(T)$. It was arbitrarily assumed that bond formation is associated with crystalline melting of the polymer, so that, based on the DSC scan for polypropylene (Fig. 3), the temperature range 140–170 °C was chosen for the calculation; further, since the nature of $F(T)$ is not known, it was assumed, for simplicity, that $K_B \rightarrow K_A$ linearly over this temperature range.

PREDICTED BEHAVIOR—INTERFACIAL MODEL

On comparing Fig. 4 for the continuum model with Figs. 8 and 9 for initial contact resistances corresponding to $K_A/K_B = 2$ and 4, respectively, it is seen that the presence of a thermal contact resistance has a major effect on the nature of the predicted temperature profiles. In fact, the greater the imposed contact resistance, the more pronounced is its effect: temperature increases more rapidly as the contact resistance is increased, particularly at the interface; moreover, a temperature gradient builds up across the interface prior to bonding and decays as bond formation proceeds.

In Figs. 10 and 11 this predicted temperature difference across the interface, ΔT, is plotted as a function of time and interfacial temperature, respectively, for the

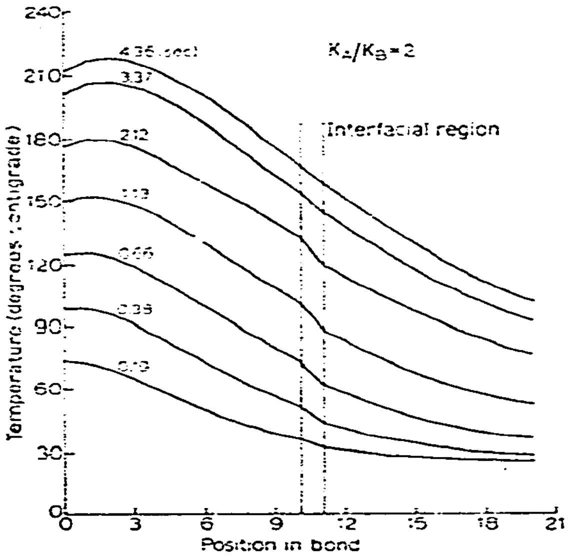

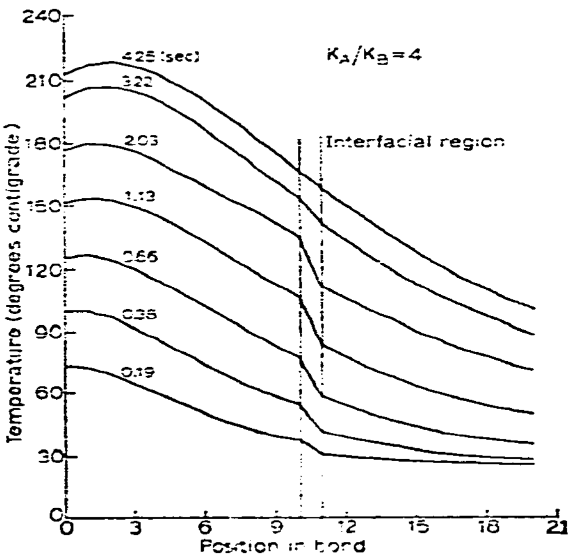

Fig. 8 (left). Predicted temperature profiles developed along central axis of bond. $K_A/K_B = 2$ prior to bond formation. Laser flux = 12 watts/cm^2.

Fig. 9 (right). Predicted temperature profiles developed along central axis of bond. $K_A/K_B = 4$ prior to bond formation. Laser flux = 12 watts/cm^2.

three values of K_A/K_B. Again, as initial contact resistance is increased, ΔT is observed to build up rapidly to higher values and, in the case of $K_A/K_B = 4$, to decay as bond formation takes place. For the bond formation models, $K_A/K_B = 2$ and 4, sharp breaks in the ΔT vs. T curves occur at 140°C, the arbitrarily selected initiation temperature for bond formation. The effect of laser flux on ΔT vs. time curves is illustrated in Fig. 12 for $K_A/K_B = 1$; as expected, the rate of increase of ΔT is greater at higher flux density and a higher maximum value is reached.

DIFFERENTIAL THERMAL SCANNING TECHNIQUE

This predicted sensitivity of ΔT, the temperature difference across the interface, to the magnitude of the initial thermal contact resistance and to the decreases in contact resistance which accompany bond formation suggested that the progress of self-adhesion might be followed by monitoring ΔT during heating. In this way it might be possible to study the effects of material variables, such as polymer molecular weight, orientation, and surface characteristics, as well as the bonding variables, pressure, temperature, and time. Accordingly, an experimental procedure was developed to test the mathematical model and the usefulness of the ΔT concept in ascertaining the influence of bonding and material variables.

Rather than trying to monitor ΔT in fibers, polymer films were used. Despite the difference in geometry and boundary conditions, the equations governing temperature as a function of position and time are the same if one restricts consider-

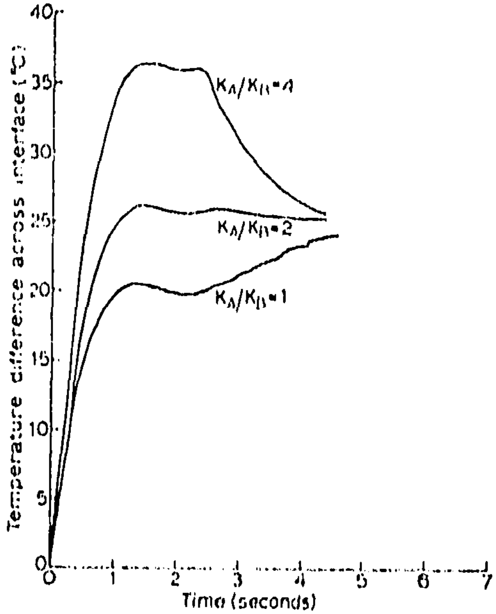

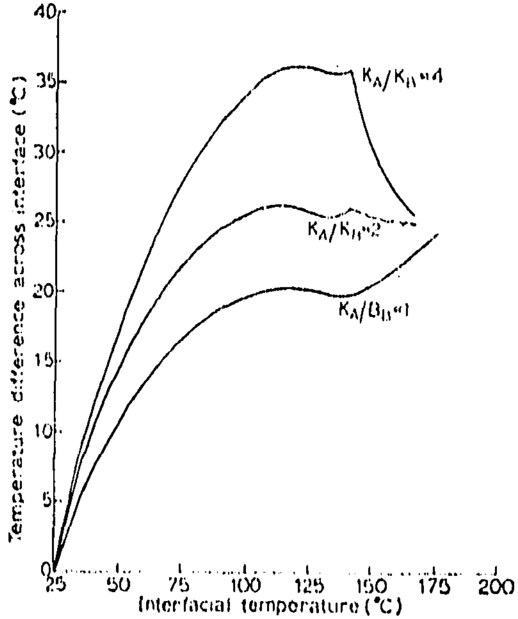

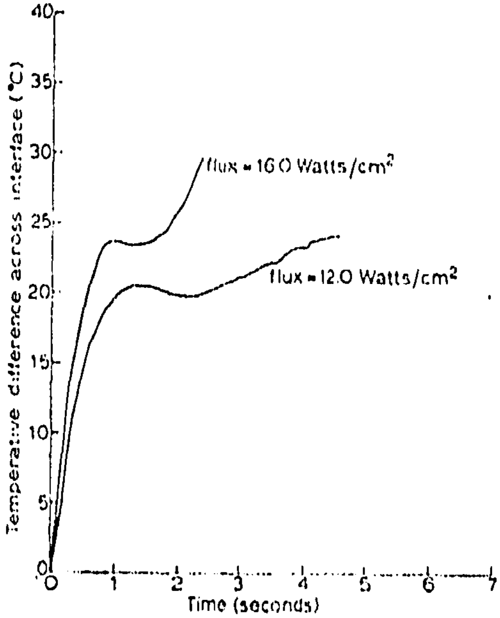

Fig. 10 (left). Predicted temperature difference across the interface as a function of time for different initial values of contact resistance. Bond formation takes place from 140 to 170 °C. Laser flux = 12 watts/cm².

Fig. 11 (centre). Predicted temperature difference across the interface as a function of temperature at the lower surface of the upper filament for different initial values of contact resistance. Bond formation takes place from 140 to 170 °C. Laser flux = 12 watts/cm².

Fig. 12 (right). Predicted effect of laser flux on the ΔT vs. time behavior for the case of no contact resistance, i.e., $K_A/K_B = 1$.

ation to an axis of symmetry. It should be justifiable, therefore, to compare the theoretical results for crossed fibers with the experimental results for films.

Fine wire thermocouples were imbedded near the surfaces of heavy polypropylene films by sandwiching the thermocouples between a thick and a very thin piece of film and bonding the composite in a hot press (Fig. 13a). Two such composites were then bonded using the CO_2 gas laser as a heat source (Fig. 13b). The thermocouples just below the contacting surfaces provide a record of the changes in both actual temperature at the lower surface of the upper film and temperature difference across the interface as laser bonding proceeds. Pressure was applied to the composites during bonding by means of a disk of Irtran, which is transparent to 10.6 μ laser radiation, loaded with brass rings of varying weights drilled out so as to pass the entire laser beam.

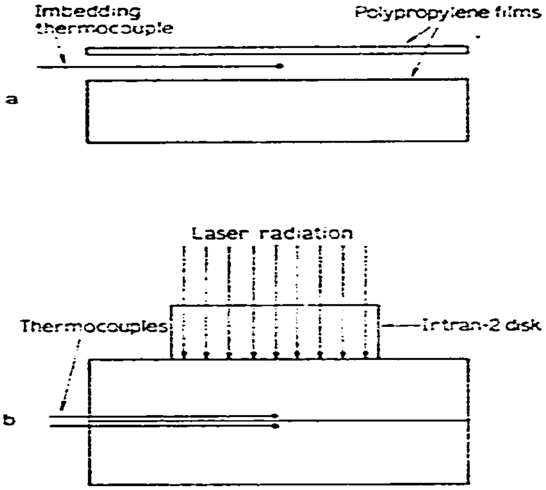

Fig. 13. Experimental procedure for monitoring ΔT, temperature difference across the interface, during bond formation: (a) sandwiching technique for imbedding thermocouples; (b) film and thermocouple arrangement during laser bonding.

CORRELATION BETWEEN EXPERIMENTAL AND MODELED BONDING

The experimental ΔT vs. t curves of Fig. 14 for films bonded at three different contact pressures are very similar to the theoretical curves of Fig. 10 for crossed filaments at three values of contact resistance generated at a comparable heating rate (laser flux). As expected, the effect of low contact pressure corresponds to that of high thermal contact resistance and vice versa, but it is rather surprising that intimate interfacial contact appears to be attained at pressures of the order of only 1 psi. It may be true, however, that, at this combination of pressure and heating rate, the contacting process does not lag behind the heating process, but that at faster heating rates, behavior resembling that predicted for $K_A/K_B > 1$ might be observed. It should be noted that the maximum in the ΔT curve for the lowest pressure, 0.13 psi, occurred at interfacial temperatures approaching 170 °C rather than 140 °C as assumed for the model. For a given heating rate, then, the interfacial region must apparently reach higher temperatures at the lower pressures before the contacting process is initiated.

The differential temperature technique was found to be sensitive to surface roughness. Figure 15 compares the ΔT vs. t behavior observed at two contact pressures and the same laser flux for relatively smooth films which had been heat-pressed against polished aluminum plates and similar films surface-roughened with emery paper. At the lower pressure, ΔT for the roughened film builds up rapidly to a very high value in the manner expected for high K_A/K_B, then decays. The interfacial temperature at the maximum was about 184°C. At the higher pressure which was apparently sufficient for intimate contact of smooth films, roughening caused the curve to assume a shape expected for an intermediate contact resistance. Thus, at the same heating rate, rough surfaces require higher threshold pressures for intimate contact than smooth ones.

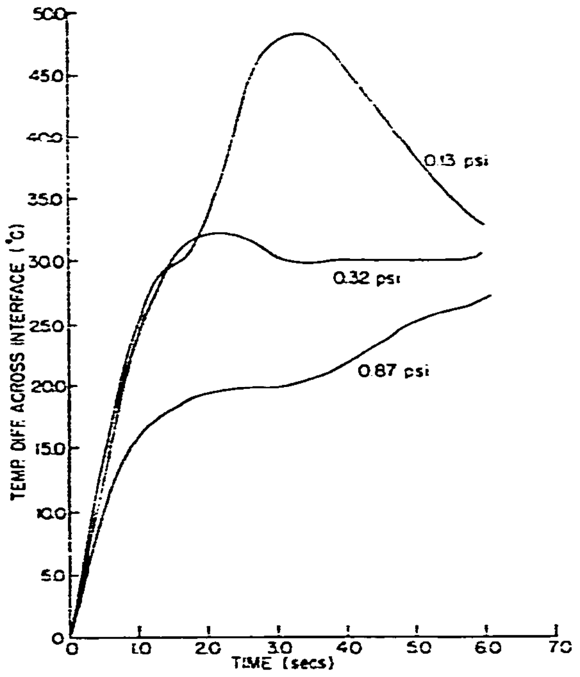

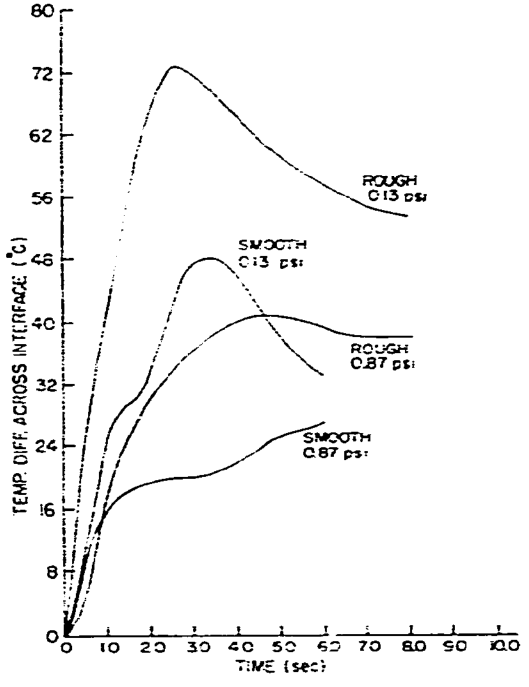

Fig. 14 (left). Experimental ΔT vs. time behavior for three different contact pressures using polypropylene films.

Fig. 15 (right). Effect of surface roughness on experimental ΔT vs. time behavior for polypropylene films.

Experimental ΔT vs. t curves (Fig. 16) corresponding to those of Fig. 12, which predict the effect of heating rate (determined by laser flux) were generated by monitoring the laser heating of prebonded film composites. In this way, the case of no contact resistance, $K_A/K_B = 1$, was simulated. Figure 16 confirms the prediction of Fig. 12 that the ΔT curves shift upward as heating rate is increased (flux at A > flux at B).

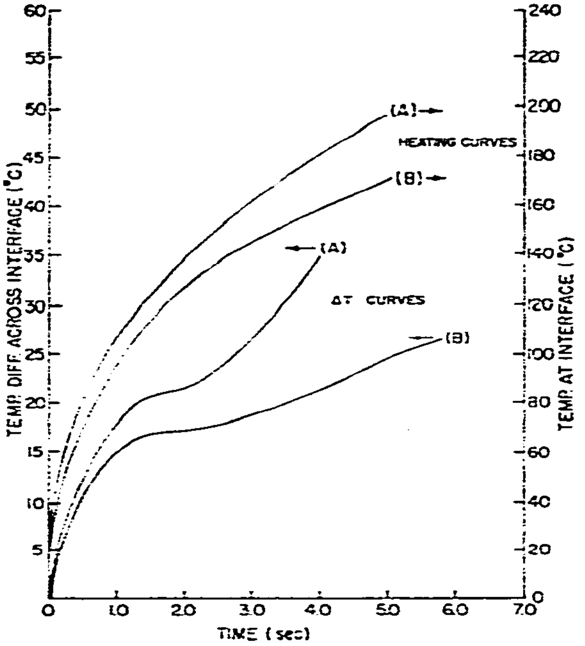

Fig. 16. Heating rate effects on experimental ΔT vs. time behavior for the case of no interface. Laser flux for curve (A) is greater than that for curve (B).

CONCLUSIONS

In view of the various assumptions made in setting up and solving the heat conduction equation, and the experimental difficulties in controlling laser heating rates and thermocouple placement, the high degree of correlation between the predictions of the model and the experimental results is gratifying. The low threshold pressure for intimate contact observed for the smooth films indicates a need for improving the sensitivity of the differential temperature measurements. Additional work is necessary, too, to determine whether differences between heating rates and contact rates are important and can be studied by this technique. As far as the model is concerned, future work should consider non-linear temperature dependence of the manner in which $K_B \to K_A$, as well as time restrictions on this process. In addition, it should be possible to adapt the model to polymers other than polypropylene and modify it for the consideration of heat sources other than the laser beam.

The experiments described herein, when interpreted in terms of the model, bear out that establishing interfacial contact is a crucial step in thermally induced polymer–polymer adhesion. Moreover, the differential temperature approach offers many possibilities for studying the interdependence of pressure, temperature, time, and material properties in controlling the contacting process in polymers. Such information is needed to facilitate selection of bonding conditions which will permit adequate fiber–fiber contact in heat-bonded non-wovens and yet minimize damage to fibers.

ACKNOWLEDGEMENT

Computations were performed on the Princeton University IBM 360/91 computer, which is supported in part by NSF grants.

REFERENCES

1 W. A. Fraser and J. C. Whitwell, *Textile Res. J.*, 41 (1971) 1003.
2 W. A. Fraser, J. C. Whitwell and B. Miller, *Textile Res. J.*, 43 (1973) 123.
3 W. A. Fraser, J. C. Whitwell and B. Miller, *Preprints, A.C.S. Meeting, Organic Coatings and Plastics Chemistry Div.*, 33 (1973) 235.
4 D. W. Peaceman and H. H. Racheford, *J. Soc. Indust. Appl. Math.*, 3 (1955) 28.